3D quantitative values of osteoradionecrosis of the jaw derived from ^{18}F-FDG PET/CT and bone SPECT/CT studies

Kazuhiro Kitajima[1] MD,
Masayuki Fujiwara[1] MD,
Tomonori Terada[2] MD,
Kazuma Noguchi[3] DDS,
Hiromitsu Kishimoto[3] DDS,
Koichiro Yamakado[1] MD

1. Department of Radiology, Hyogo Medical University, Nishinomiya, Japan,
2. Department of Otolaryngology, Head and Neck Surgery, Hyogo Medical University, Nishinomiya, Japan,
3. Department of Oral & Maxillofacial Surgery, Hyogo Medical University, Nishinomiya, Japan

Keywords: Osteoradionecrosis (ORN) - ^{18}F-FDG PET/CT - SPECT/CT - Standardized uptake value (SUV)

Corresponding author:
Kazuhiro Kitajima MD, Department of Radiology, Hyogo Medical University, Nishinomiya, Hyogo, Japan, 1-1 Mukogawa-cho, Nishinomiya, Hyogo 663-8501 Japan
Phone: 81-798-45-6883
Fax: 81-798-45-6262
kazu10041976@yahoo.co.jp

Received:
31 January 2025
Accepted revised:
31 March 2025

Abstract

Objective: To investigate the clinical utility of the 3D quantitative values derived from fluorine-18-fluorodeoxyglucose positron emission tomography/computed tomography (^{18}F-FDG PET/CT) and bone single-photon computed tomography-computed tomography (SPECT/CT) for the diagnosis of osteoradionecrosis (ORN) of the jaw. **Subjects and Methods:** Thirty four patients with head and neck cancer who had a history of radiotherapy and clinically diagnosed as ORN and who undertaken ^{18}F-FDG PET/CT (n=23) or quantitative bone SPECT/CT (n=11) were enrolled. Standardized uptake values (SUV), including maximum SUV (SUVmax), peak SUV (SUVpeak), and mean SUV (SUVmean), as well as metabolic lesion volume (MLV), representing total volume above threshold, and total lesion uptake (TLU), calculated as MLV×SUVmean were determined. **Results:** In ^{18}F-FDG PET/CT results, mean values (range) of SUVmax, SUVpeak, SUVmean, MLV, and TLU of 24 lesions were 6.72±2.62 (3.67~14.36), 5.25±2.05 (2.46~10.88), 3.77±1.33 (1.74~7.69), 11.49±9.61 (1.54~43.14), and 49.07±59.26 (4.44~271.05), respectively. In quantitative bone SPECT/CT results, mean values (range) of SUVmax, SUVpeak, SUVmean, MLV, and TLU of 16 lesions were 5.26±0.89 (3.71~7.07), 4.62±0.78 (3.09~6.02), 3.44±0.46 (2.68~4.32), 14.45±9.93 (1.48~33.32), and 49.72±35.51 (4.60~127.86), respectively. **Conclusion:** As objective and reliable indicators, 3D quantitative values (SUV and volume) derived from ^{18}F-FDG PET/CT and quantitative bone SPECT/CT results are useful for evaluation of the disease activity of ORN of the jaw.

Hell J Nucl Med 2025; 28(1): 8-13 *Epub ahead of print: 7 April 2025* *Published online: 30 April 2025*

Introduction

While being an integral part of the multidisciplinary management of head and neck cancer, radiotherapy (RT) might cause various complications-of which mandibular osteoradionecrosis (ORN) is one of the most feared. Published data suggest that the prevalence of this condition following RT varies from 2% to 9%, with the main risk factors being age>55 years [1, 2], active smoker at diagnosis [3] and RT doses>60Gy [4]. In general, ORN can be defined as an area of exposed devitalized irradiated bone that fails to heal over a period of three months without signs of recurrent or residual malignancy [5, 6]. Bone necrosis is a common characteristic of ORN and has clinical signs and symptoms [7]. The pathogenesis of ORN is complex and includes local inflammation, damage to vascular supply as a result of surgery or obliterative endarteritis, and altered bone healing accompanied by an increased susceptibility to infections [8, 9].

Molecular imaging such as bone scintigraphy and fluorine-18-fluorodeoxyglucose positron emission tomography/computed tomography (^{18}F-FDG PET/CT) has been reported to be useful for detecting ORN of the jaw after RT for head and neck cancer [10-12]. Three groups have introduced the 3D quantitative values including standardized uptake value (SUV) derived from bone single-photon emission computed tomography/computed tomography (SPECT/CT) and ^{18}F-FDG PET/CT examinations in the ORN of the jaw [13-15]. The purpose of our study is to evaluate the usefulness of 3D quantitative values (SUV and volume) derived from bone SPECT/CT and ^{18}F-FDG PET/CT studies in the ORN of the jaw after RT for head and neck cancer.

Subjects and Methods

Patients

This was conducted as a retrospective study following approval from the Ethics Com-

mittee of this institution (No. 3144). Thirty four patients with head and neck cancer who had a history of RT and suspected ORN according to the various clinical and imaging examinations had undertaken ^{18}F-FDG PET/CT (23 patients) or quantitative bone SPECT/CT (11 patients) examinations between January 2010 and January 2024. Patients and lesion characteristics are shown in Table 1.

Table 1. *Patient characteristics and demographics.*

	Number	%
Sex		
Male	24	70.6
Female	10	29.4
Age		
Mean±SD	67.5±10.7	
Range	49-85	
Location		
Maxilla	6	15.0
Mandible	34	85.0
Primary tumor		
Oropharyngeal	17	50.0
Nasopharygeal	5	14.7
Tongue	4	11.8
Laryngeal	2	5.9
Gingival	2	5.9
Hypopharygeal	1	2.9
Buccal mucosa	1	2.9
Parotid gland	1	2.9
Floor of the mouth	1	2.9
Previous treatment		
Chemoradiation	20	58.8
Surgery followed by chemoradiotherapy	11	27.5
Chemoradiotherapy followed by surgery	2	5.0
Radiotherapy	1	2.5
Radiation dose (Gy)		
Median	66	
Range	60-72	
Interval between last radiotherapy and detection of abnormality (months)		
Mean±SD	66.6±53.1	
Range	18-276	

SD: standard deviation

^{18}F-FDG PET/CT

Our institution has four PET/CT scanning devices available (Gemini GXL16, Gemini TF64, Ingenuity TF: Philips Medical Systems, Eindhoven, The Netherlands; Discovery IQ: GE Healthcare, Waukesha, WI, USA), which were used for ^{18}F-FDG PET/CT examinations of the present patients. Prior to scanning, each was asked to fast for five hours, then blood glucose measurement was performed immediately before ^{18}F-FDG injection (4.0MBq/kg body weight for GXL16, 3.0MBq/kg for TF64, 3.7MBq/kg body weight for Ingenuity TF and Discovery IQ), with <160mg/dL noted in all. Static emission images were then obtained approximately 60 minutes following the injection. Helical CT scan imaging was performed from the top of the head to mid-thigh with the following parameters used for attenuation correction and anatomic localization: tube voltage 120kV (all four scanners), effective tube current auto-mA up to 120mA (GXL16), 100mA (TF64), 155mA (Ingenuity TF) or 15-390mA (Smart mA: noise index 25) (Discovery IQ), gantry speed 0.5 rotations/second, detector configuration 16×1.5mm (GXL16), 64×0.625mm (TF64, Ingenuity TF), or 16×1.25mm (Discovery IQ), slice thickness 2mm, and transverse field of view 600mm (GXL16, TF64, Ingenuity TF) or 700mm (Discovery IQ). Following the CT examination, PET imaging was immediately performed from head to mid-thigh for 90 seconds (GXL16, TF64, Ingenuity TF) or 180 seconds (Discovery IQ) for each bed position in three-dimensional mode. Normal breathing was allowed during PET scanning. For GXL16 examinations, attenuation-corrected PET images were reconstructed using a line-of-response row-action maximum likelihood algorithm, while for those performed with the TF64 and Ingenuity, an ordered-subset expectation maximization (OSEM) iterative reconstruction algorithm (33 subsets, three iterations), and

with the Discovery IQ Q.Clear, a block sequential regularized expectation maximization (BSREM) iterative reconstruction algorithm (β=400) were utilized.

The ^{18}F-FDG PET/CT images were retrospectively reviewed by a nuclear medicine expert with board certification and 16 years of oncologic ^{18}F-FDG PET/CT experience. During analysis of the present patient findings, performed using the GI-PET software package (AZE Co., Ltd., Tokyo, Japan), which can harmonize SUV obtained with different PET/CT systems using phantom data [16], knowledge of other imaging results, or clinical or histopathologic data were not provided. The maximum concentration in the target lesion (injected dose/ body weight) was used to define SUVmax, while calculation of SUVpeak was done with use of a volume region of interest (ROI) sized 1.2cm in diameter placed on the hottest site. Fluorine-18-FDG-avid tumor volume was employed to define metabolic lesion volume (MLV), with 40% of SUVmax used as the margin threshold. Calculation of total lesion uptake (TLU) was then performed, as follows: SUVmean×MLV, with SUVmean representing mean SUV value.

Bone SPECT/CT

Three to four hours after intravenous administration of technetium-99m-hydroxymethylene diphosphonate (^{99m}Tc-HMDP), planar bone scintigraphy was performed with a 555 MBq dose using a SPECT/CT scanner (NM/CT670; GE Healthcare, Pittsburgh, Pa) equipped with a low-energy high-resolution collimator. Immediately after a planar image of the jaw area was obtained, quantitative SPECT/CT images were acquired using a hybrid system. First, CT images were obtained using the following parameters: tube voltage 120 kV, tube current 60-210mA with "autoMa" function and 20 noise level, X-ray collimation 20mm (16×1.25mm), table speed 37mm/second, table feed 18.75mm/rotation, tube rotation time 0.5 seconds, pitch 0.938:1, and a 512×512 matrix. Those images were reconstructed into 2.5-mm thick sections with use of an adaptive statistical iterative reconstruction algorithm (ASiR; GE Healthcare). Thereafter, SPECT images were acquired using the following parameters: energy peak 140 KeV with a 20% window (126-154KeV), step-and-shot mode acquisition (16 seconds per step, 60 steps per detector) with a 3° angular increment, and body contour scanning option. An extra window for scatter correction was set at 120KeV with a 10% window (115-125KeV). The SPECT images were then reconstructed by use of an iterative ordered subset expectation maximization algorithm (two iterations, 10 subsets) with CT-based attenuation correction, scatter correction, and resolution recovery using the software package supplied by the vendor (Volumetrix MI; GE Healthcare). A post-reconstruction filter was applied (Butterworth filter, frequency of 0.48, order of 10). Images were reconstructed with a 128×128 matrix, section thickness of 2.95mm, and zoom factor of 1.5.

Delineation of volume of interest (VOI) was performed by the consensus of a radiological technologist and a board-certified nuclear medicine expert with 15 years of oncologic nuclear medicine experience and without knowledge of the other imaging results, or clinical or histopathologic data for the present patients, using GI-BONE, a commercially available software package (AZE Co., Ltd., Tokyo Japan), which is used to present statistics for various SUVs, SUVmax, which represents the single greatest point of metabolic activity within the lesion, and SUVpeak, defined as the average concentration of activity within a 1cm^3 spherical VOI centered on the "hottest focus" within the lesion, as well as MLV, defined as lesion volume with uptake, and TLU, calculated as SUVmean × MLV [17]. The average SUV value that showed 40% or more of SUVmax in the VOI was defined as SUVmean.

Results

Twenty three patients with 24 ORN lesions received ^{18}F-FDG PET/CT scans and 11 patients with 16 ORN lesions received quantitative bone SPECT/CT examinations.

In ^{18}F-FDG PET/CT results, mean values (range) of SUVmax, SUVpeak, SUVmean, MLV, and TLU of 24 ORN lesions were 6.72±2.62 (3.67~14.36), 5.25±2.05 (2.46~10.88), 3.77±1.33 (1.74~7.69), 11.49±9.61 (1.54~43.14), and 49.07±59.26 (4.44~271.05), respectively. One representative case is shown in Figure 1.

In quantitative bone SPECT/CT results, mean values (range) of SUVmax, SUVpeak, SUVmean, MLV, and TLU of 16 ORN lesions were 5.26±0.89 (3.71~7.07), 4.62±0.78 (3.09~6.02), 3.44±0.46 (2.68~4.32), 14.45±9.93 (1.48~33.32), and 49.72± 35.51 (4.60~127.86), respectively. One representative case is shown in Figure 2.

Discussion

The occurrence of ORN is not time dependent; hence, it may become evident even years after RT [18]. Osteoradionecrosis typically develops with a small incomplete wound healing and a small area of mucosal collapse with exposure of the underlying bone and reactive inflammatory granulation tissue, by triggers such as tooth extraction. This means ORN begins with traumatic invasion into the injured devitalized bone with mucosal collapse. As ORN progresses, patients often develop chronic inflammatory trismus, neuropathic pain, chronic drainage, and pathological fracture.

Fluorine-18-FDG PET/CT and bone scintigraphy has been reported to be useful for detecting ORN of the jaw after RT for head and neck cancer [10-12]. Ogura et al. (2019) [11] reported 100% sensitivity (7/7) of bone scintigraphy. Miyamoto et al. (2021) [12] reported 85.7% sensitivity (30/35) of ^{18}F-FDG-PET/CT and 94.4% sensitivity (17/18) of bone scintigraphy. Fluorine-18-FDG is known to accumulate in areas of inflammation, due to uptake by the inflammation cells. Yamada et al. (1995) [19] showed marked ^{18}F-FDG uptake increase in the presence of hypoxia and inflammatory mediators. The presence of increased uptake in the bone scintigraphy depends on osteoblastic activity and skeletal vascularity [20]. Fluorine-18-FDG PET/CT and bone scintigraphy are sensitive indicators of altered osteoblastic activity, but local disturbances in vascular perfusion, clearance rate, per-

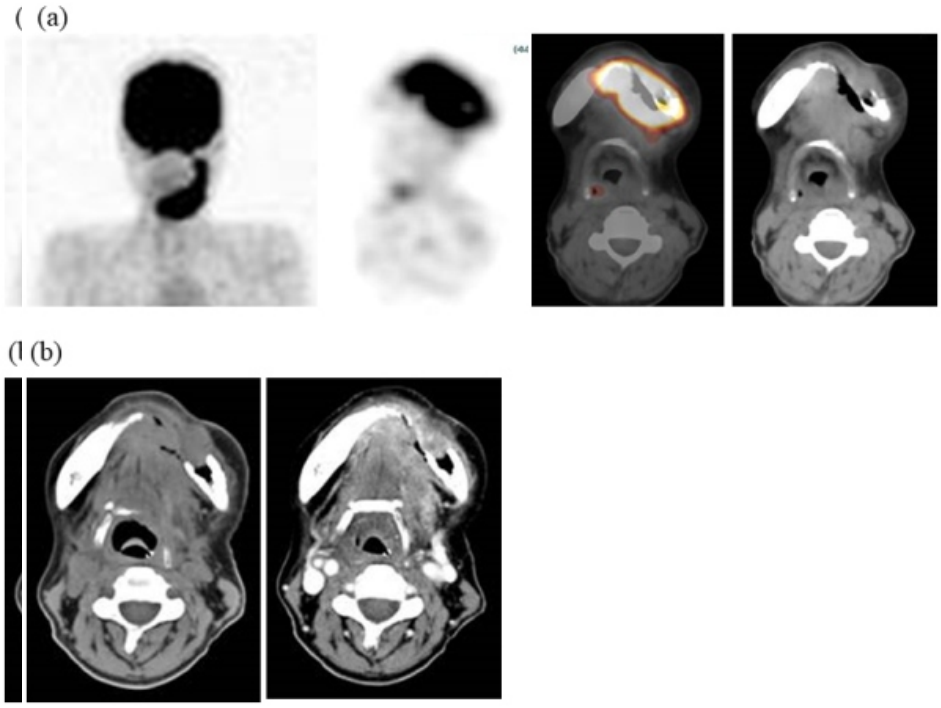

Figure 1. A 58-year-old female with mandibular osteoradionecrosis, who previously received chemoradiotherapy for tongue cancer 43 months ago. (a) ^{18}F-FDG PET/CT shows strong ^{18}F-FDG uptake and bone destruction with gas in the mandible. Maximum SUV, SUVpeak, SUVmean, MLV, and TLU of the lesion are 11.29, 9.17, 6.28, 43.1, and 271.1 respectively. (b) CT shows an enhancing soft-tissue mass with bone destruction and gas in the mandible.

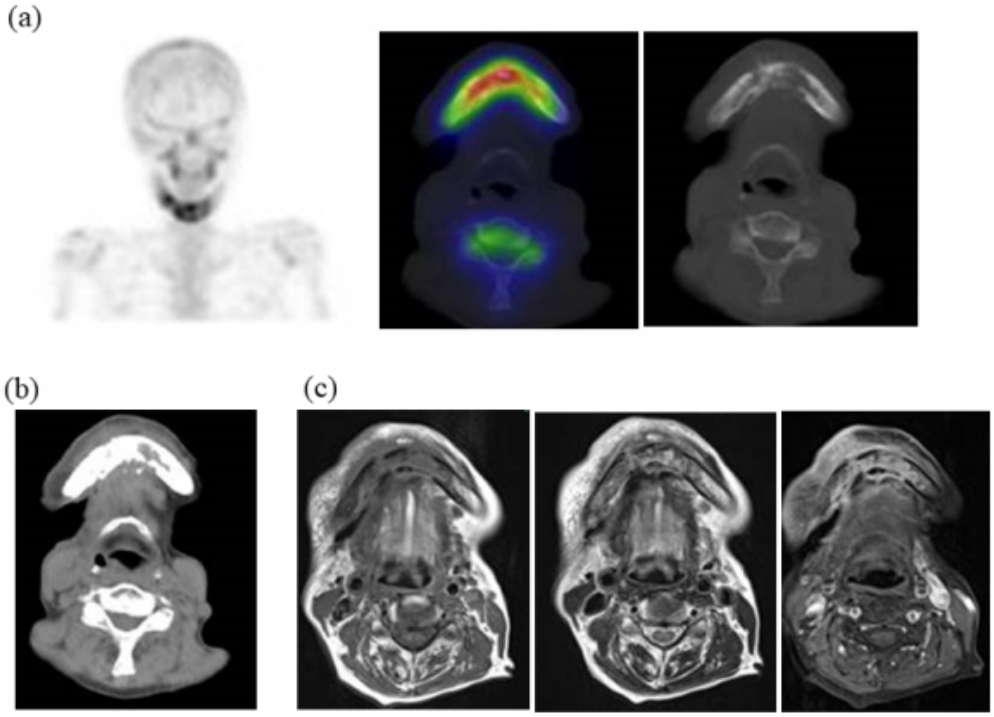

Figure 2. A 79-year-old female with mandibular osteoradionecr osis, who previously received chemoradiotherapy for oropharyngeal cancer 20 months ago. (a) Bone SPECT/CT shows medium uptake and combined osteolytic and sclerotic change in the mandible. Maximum SUV, SUVpeak, SUVmean, MLV, and TLU of the lesion are 6.46, 5.49, 3.84, 33.32, and 127.86 respectively. (b) CT shows combined osteolytic and sclerotic lesion in the mandible. (c) MRI shows decreased marrow signal intensity on T1-weighted image and heterogeneous increased marrow signal intensity on T2-weighted image with heterogeneous enhancement in the mandible.

meability, and chemical binding also affect imaging [21].

Three groups have introduced the 3D quantitative values (SUV and volume) derived from ^{18}F-FDG PET/CT and quantitative bone SPECT/CT examinations in the ORN of the jaw [13-15]. In the ^{18}F-FDG PET/CT study of 46 patients with ORN of the jaw, Alhilali et al. (2014) [13] reported that SUVmax showed mean of 5.3 (range of 1.7-9.2) and SUVmean showed mean of 4.3 (range of 2.2-7.5). In the ^{18}F-FDG PET/CT study of 29 patients with ORN of the jaw, Meerwein et al. (2018) [14] reported that mean±SD of SUVmax, MLV, and TLU were 5.96±2.32, 7.51±7.53, and 27.15±28.74, respectively. In the quantitative bone SPECT/CT of 12 patients with ORN of the jaw, Minami et al. (2021) [15] reported that SUVpeak showed mean±SD of 6.7±2.1 and range of 4.0-11.4, and SUVmean showed mean±SD of 6.3±1.8 and range of 4.3-10.1, respectively. Standardized uptake values in our series are similar to these previous reports although our SUVmax on ^{18}F-FDG PET/CT scan is slightly higher than previous reports' SUVmax [13, 14] and our SUVmax on bone quantitative SPECT/CT scan is slightly lower than previous reports' SUVmax [15].

Typical osseous findings of ORN on CT include cortical disruption, disorganization of trabeculation, and osseous fragmentation [12]. A possible explanation for the bone sclerosing mechanisms is that the damage from radiation to the bone tissue continues to stimulate bone cells [22]. The damage affects osteocytes and activates osteoblasts, which cause reactive bone consolidation, particularly in the cancellous bone area. Radiotherapy reduces not only the proliferation of bone marrow and periosteal and endothelial cells but also the production of the extracellular matrix, particularly the collagen.

Magnetic resonance imaging shows that the damage to the bone marrow by RT continued even after the long-term asymptomatic phase. Even if there are no clinical symptoms of ORN, the bone marrow is considered abnormal for a long time after RT. Considering the CT images, the consolidated bone region would have devitalized or reduced vitality, possibly fibrosis with lower blood supply. Partial bone resorption and reactive fibrosis showed a mixed image of bone consolidation (low intensities on T1-weighed imaging (T1 WI) and heterogeneous hyper-intensities on T2-weighted imaging (T2WI)), as Kaneda has previously suggested [21, 23]. Moreover, the homogeneous hyper-intensities of T2WI may be mild bone marrow inflammation considering the clinical symptoms of ORN. From a clinical point of view, tooth extraction within the radiation field should be performed with caution at any time after RT. If abnormal bone marrow is invaded by triggers, the symptoms of ORN would change from the chronic inflammation phase to the acute inflammation phase. Tooth extraction before RT is recommended, but it does not prevent ORN; the essence of ORN is devitalized bone. Considering soft tissue, CT and MRI often show inflammation in the surrounding masticatory muscles, and MRI can confirm the inflammatory symptoms around the masticatory muscles [24].

This study has several limitations, including the relatively small number of patients. An additional limitation is lack of comparisons with CT/MRI imaging findings due to few cases of CT/MRI scans.

In conclusion, as objective and reliable indicators, 3D quantitative values (SUV and volume) derived from ^{18}F-FDG PET/CT and quantitative bone SPECT/CT results are useful for evaluation of the disease activity of ORN of the jaw.

The authors declare that they have no conflicts of interest

Funding Source

This study was supported by a Grant-in-Aid from the Ministry of Education, Culture, Sports, Science, and Technology of Japan (No. 22K07757).

Bibliography

1. Reuther T, Schuster T, Mende U, Kübler A. Osteoradionecrosis of the jaws as a side effect of radiotherapy of head and neck tumour patients-a report of a thirty year retrospective review. *Int J Oral Maxillofac Surg* 2003; 32: 289-95.
2. Pitak-Arnnop P, Sader R, Dhanuthai K et al. Management of osteoradionecrosis of the jaws: an analysis of evidence. *Eur J Surg Oncol* 2008; 34: 1123-34.
3. Möring MM, Mast H, Wolvius EB et al. Osteoradionecrosis after postoperative radiotherapy for oral cav ity cancer: a retrospective cohort study. *Oral Oncol* 2022; 133: 106056.
4. Chang CT, Liu SP, Muo CH et al. The impact of dental therapy timelines and irradiation dosages on osteoradionecrosis in oral cancer patients: a population-based cohort study. *Oral Oncol* 2022; 128: 105827.
5. Marx RE. A new concept in the treatment of osteoradionecrosis. *J Oral Maxillofac Surg* 1983; 41: 351-7.
6. Jacobson AS, Buchbinder D, Hu K, Urken ML. Paradigm shifts in the management of osteoradionecrosis of the mandible. *Oral Oncol* 2010; 46: 795-801.
7. Nabil S, Samman N. Incidence and prevention of osteoradionecrosis after dental extraction in irradiated patients: A systematic review. *Int J Oral Maxillofac Surg* 2011; 40: 229-43.
8. Wang CC, Cheng MH, Hao SP et al. Osteoradionecrosis with combined mandibulotomy and marginal mandibulectomy. *Laryngo scope* 2005; 115: 1963-7.
9. Davis DD, Hanley ME, Cooper JS. Osteoradionecrosis. Treasure Island: StatPearls; 2022.
10. Deshpande SS, Thakur MH, Dholam K et al. Osteoradionecrosis of the mandible: through a radiologist's eyes. *Clin Radiol* 2015; 70: 197-205.
11. Ogura I, Sasaki Y, Sue M et al. ^{99m}Tc-hydroxymethylene diphosphonate scintigraphy, computed tomography, and magnetic resonance imaging of osteonecrosis in the mandible: Osteoradionecrosis versus medication-related osteonecrosis of the jaw. *Imaging Sci Dent* 2019; 49: 53-8.
12. Miyamoto I, Tanaka R, Kogi S et al. Clinical diagnostic imaging study of osteoradionecrosis of the jaw: A Retrospective Study. *J Clin Med* 2021; 10: 4704
13. Alhilali L, Reynolds AR, Fakhran S. Osteoradionecrosis after radiation therapy for head and neck cancer: differentiation from recurrent disease with CT and PET/CT imaging. *Am J Neuroradiol* 2014; 35: 1405-11
14. Meerwein CM, Nakadate M, Stolzmann P et al. Contrast-enhanced ^{18}F-FDG-PET/CT for Differentiating Tumour and Radionecrosis in Head and Neck Cancer: Our experience in 37 Patients. *Clin Otolaryngol* 2018; 43: 1594-9.
15. Minami Y, Ogura I. Bone single-photon emission computed tomography-CT peak standardized uptake value for chronic osteomyelitis, osteoradionecrosis and medication-related osteonecrosis of the jaw. *J Med Imaging Radiat Oncol* 2021; 65: 160-5
16. Kitajima K, Nakatani K, Yamaguchi K et al. Response to neoadjuvant chemotherapy for breast cancer judged by PERCIST- multicenter study in Japan. *Eur J Nucl Med Mol Imaging* 2018; 45: 1661-71.
17. Moridera K, Kitajima K, Yoshikawa K et al. Usefulness of quantitative bone SPECT/CT for medication-related osteonecrosis of the jaw in clinical settings. *Jpn J Radiol* 2022; 40: 492-9.

18. Reuther T, Schuster T, Mende U, Kübler A. Osteoradionecrosis of the jaws as a side effect of radiotherapy of head and neck tumor patients-a report of a thirty year retrospective review. *Int J Oral Maxillofac Surg* 2003; 32: 289-95.
19. Yamada S, Kubota K, Kubota R et al. High accumulation of fluorine-18-fluorodeoxyglucose in turpentine-induced inflammatory tissue. *J Nucl Med* 1995; 36: 1301-6.
20. Arce K, Assael LA, Weissman JL, Markiewicz MR. Imaging findings in bisphosphonate-related osteonecrosis of jaws. *J Oral Maxillofac Surg* 2009; 67: 75-84.
21. Kaneda T, Minami M, Ozawa K et al. Magnetic resonance imaging of osteomyelitis in the mandible. Comparative study with other radiologic modalities. *Oral Surg Oral Med Oral Pathol Oral Radiol Endod* 1995; 79: 634-40.
22. Alhilali L, Reynolds AR, Fakhran S. Osteoradionecrosis after radiation therapy for head and neck cancer: Differentiation from recurrent disease with CT and PET/CT imaging. *Am J Neuroradiol* 2014; 35: 1405-11.
23. Ariji Y, Izumi M, Gotoh M et al. MRI features of mandibular osteomyelitis: Practical criteria based on an association with conventional radiography features and clinical classification. *Oral Surg Oral Med Oral Pathol Oral Radiol Endod* 2008; 105: 503-11.
24. Chong J, Hinckley LK, Ginsberg LE. Masticator space abnormalities associated with mandibular osteoradionecrosis: MR and CT findings in five patients. *Am J Neuroradiol* 2000; 21: 175-8.